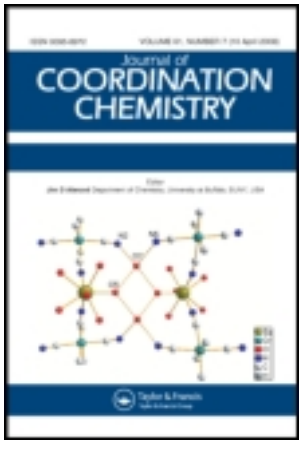

Journal of Coordination Chemistry
Publication details, including instructions for authors and subscription information:
http://www.tandfonline.com/loi/gcoo20

Two zinc(II) complexes based on indole-3-acetic acid: crystal structures, fluorescence sensors, and ion exchange with mercury(II)

Xuling Xue [a], Yanyan Zhu [a], Bo Xiao [b], Lu Liu [a] & Hong Xu [a]

[a] Department of Chemistry, Zhengzhou University, Zhengzhou, Henan 450052, P.R. China

[b] Material and Chemical Engineering College, Zhengzhou University of Light Industry, Zhengzhou, Henan 450002, P.R. China

Published online: 19 Aug 2011.

To cite this article: Xuling Xue, Yanyan Zhu, Bo Xiao, Lu Liu & Hong Xu (2011) Two zinc(II) complexes based on indole-3-acetic acid: crystal structures, fluorescence sensors, and ion exchange with mercury(II), Journal of Coordination Chemistry, 64:16, 2923-2935, DOI: 10.1080/00958972.2011.609277

To link to this article: http://dx.doi.org/10.1080/00958972.2011.609277

Journal of Coordination Chemistry
Vol. 64, No. 16, 20 August 2011, 2923–2935

Two zinc(II) complexes based on indole-3-acetic acid: crystal structures, fluorescence sensors, and ion exchange with mercury(II)

XULING XUE†, YANYAN ZHU†, BO XIAO‡, LU LIU† and HONG XU*†

†Department of Chemistry, Zhengzhou University, Zhengzhou, Henan 450052, P.R. China
‡Material and Chemical Engineering College, Zhengzhou University of Light Industry, Zhengzhou, Henan 450002, P.R. China

(*Received 24 February 2011; in final form 23 June 2011*)

Two new coordination complexes, $[Zn(IA)_2(phen)]$ (**1**) and $[Zn(IA)_2(4,4'\text{-bipy})]_n \cdot C_2H_5OH$ (**2**) (IAH = indole-3-acetic acid, phen = 1,10-phenanthroline, 4,4′-bipy = 4,4′-bipyridine), have been prepared and characterized by single-crystal X-ray diffraction. Complex **1** is mononuclear and **2** presents a 1-D zigzag chain, in which 4,4′-bipy connects the Zn(II) ions. Both complexes show fluorescence emissions and exhibit fluorescence quenching when Hg^{2+} ions are present. ICP, EDS, and SEM experiments reveal that zinc in both complexes can be exchanged by toxic mercury ions.

Keywords: Crystal structure; Indole-3-acetic acid; Fluorescence; Cation exchange

1. Introduction

Many metals exist in the form of coordination compounds in living organisms and play roles in life. For example, heme is an iron complex; chlorophyll is a magnesium complex; vitamin B_{12} is a cobalt complex. Construction of new complexes with biological activity has been a great focus. There also exist many heavy metal elements which are deadly to organisms.

Mercury is highly toxic with accumulative and persistent character in the environment, even at very low concentrations [1]. Thus, detecting the distribution and content of mercury is important to prevent risk. Development of methods for the detection of mercury with high efficiency is important. Several techniques, such as colorimetric [2], fluorogenic [3, 4], redox-active [5, 6] methods, and chemodosimeter, have been reported. These methods offer good limits of detection and wide linear ranges. However, most of these techniques necessitate the use of sophisticated apparatus and intricate preparation. Among the various methods to monitor mercury ions under environmental conditions, fluorescence chemosensors are widely regarded as

*Corresponding author. Email: xuhong@zzu.edu.cn

Journal of Coordination Chemistry
ISSN 0095-8972 print/ISSN 1029-0389 online © 2011 Taylor & Francis
DOI: 10.1080/00958972.2011.609277

one of the most effective ways with visual effects, greater sensitivity, and simple equipment. A number of fluorescence Hg^{2+} sensors, such as small molecules [7], gold nanoparticles [8], DNAzymes [9], protein [10], oligonucleotide [11], and polymers [12], have been reported. However, most of these sensors suffer from poor water solubility and require complex processes, expensive instrumentation and are even harmful to the environment [13–15]. Therefore, development of accessible and new Hg fluorescent sensors is still very important.

In this work, we present two new complexes, $[Zn(IA)_2(phen)]$ (**1**) and $[Zn(IA)_2(4,4'\text{-bipy})]_n \cdot C_2H_5OH$ (**2**), which are assembled from Zn^{2+} and indole-3-acetic acid (IAH), phen, and 4,4′-bipy. Both can detect Hg^{2+} with high selectivity and sensitivity, and also introduce the useful trace element zinc and IAH, beneficial for the growth of the plants. Through ICP and EDS experiments, we find that Zn(II) in **1** and **2** could be exchanged for Hg^{2+}.

2. Experimental

2.1. *General information and materials*

IAH, phen, and 4,4′-bipy were of reagent quality obtained from commercial sources and used without purification. IR data were recorded on a BRUKER TENSOR 27 spectrophotometer with KBr pellets from 400 to 4000 cm^{-1}. Elemental analyses (C, H, and N) were carried out on a FLASH EA 1112 elemental analyzer. Luminescence spectra were measured on powder samples at room temperature using a F-4500 HITACHI Fluorescence Spectrophotometer. Metal ion was measured by an IRIS Advantage ICP (TJA, USA). Field emission scanning electron microscopy (SEM) and energy-dispersive X-ray spectrometry (EDS) were conducted on a JSM-6490 scanning electron microscope.

2.2. *Synthesis of the complexes*

2.2.1. Synthesis of 1. An ethanol solution (2 mL) containing IAH (0.02 mmol), which was adjusted to pH = 7.5 using 0.01 mol dm^{-3} NaOH, was added into an aqueous solution of $ZnSO_4$ (0.01 mmol) with stirring at room temperature. After 3 h, an ethanol solution of 1,10-phenanthroline (0.01 mmol) was added. The mixture was stirred for a further 30 min and filtered. Pale-yellow block crystals were generated in 2 weeks at room temperature after the filtrate was quietly placed in a dark environment. Yield is 38%. Anal. Calcd for $C_{32}H_{24}N_4O_4Zn$ (%):C, 64.66; N, 9.43; H, 4.04. Found (%): C, 64.62; N, 9.38; H, 4.08. IR (KBr, cm^{-1}): 3395(m), 3172(m), 1594(s), 1457(w), 1426(m), 1381(m), 1231(w), 940(w), 846(s), 762(m), 745(s), 723(s), 648(w).

2.2.2. Synthesis of 2. The synthesis of **2** is similar to that of **1** except for 4,4′-bipy substituting for phen. Pale-yellow block crystals suitable for X-ray diffraction were obtained in 7 days at room temperature in 45% yield. Anal. Calcd for $C_{32}H_{30}N_4O_5Zn$ (%): C, 62.34; N, 9.09; H, 4.87. Found (%): C, 62.36; N, 9.07;

H, 4.80. IR (KBr, cm^{-1}): 3208(m), 1612(s), 1536(m), 1490(m), 1417(s), 1216(m), 1015(m), 981(w), 858(w), 809(m), 727(w), 643(m), 619(s).

2.3. *X-ray crystallography*

The data for **1** and **2** were collected on a Rigaku Saturn 724 detector with graphite-monochromatic Mo-Kα radiation ($\lambda = 0.71073$ Å). A single crystal suitable for X-ray diffraction was selected and mounted on a glass fiber at 291(2) K. The data were integrated using the CrystalClear-SM 1.3.6 SP3r6 program with intensities corrected for Lorentz-polarization effects [16]. Absorption corrections were applied by using the MULTISCAN program. The non-hydrogen atoms were refined anisotropically. Hydrogens were generated geometrically and hydrogens bonded to carbons were allowed to ride on their parent carbon. The final cycle of full-matrix least-squares refinement was based on observed reflections and variable parameters. All calculations were performed using the SHELX 97 Crystallographic software package [17]. Crystallographic parameters and structural refinement for **1** and **2** are summarized in table 1. Selected bond lengths and angles of the two complexes are listed in table 2.

2.4. *Selective activities of 1 and 2*

Standard water solutions of 1.0×10^{-5} mol dm^{-3} metal ions were prepared from chloride salts of Na^+, K^+, Mg^{2+}, Ca^{2+}, Cr^{3+}, Mn^{2+}, Fe^{3+}, Co^{2+}, Ni^{2+}, Cu^{2+}, Cd^{2+},

Table 1. Crystal data and structural refinement of **1** and **2**.

Complex	**1**	**2**
Empirical formula	$C_{32}H_{24}N_4O_4Zn$	$C_{32}H_{30}N_4O_5Zn$
Formula weight	593.94	615.97
Temperature (K)	291(2)	291(2)
Crystal system	Monoclinic	Monoclinic
Space group	$P2_1/c$	$P2_1/c$
Unit cell dimensions (Å, °)		
a	12.300(5)	18.024(4)
b	12.552(5)	8.8120(18)
c	17.673(7)	18.516(4)
α	90	90
β	105.971(6)	98.37(3)
γ	90	90
Volume (Å^3), Z	2623.3(18), 4	2909.5(10), 4
Calculated density (Mg m^{-3})	1.504	1.406
Absorption coefficient (mm^{-1})	0.984	0.892
F(000)	1224	1280
Crystal sizes (mm^3)	$0.22 \times 0.21 \times 0.18$	$0.25 \times 0.22 \times 0.16$
R(int)	0.0832	0.0419
Data/restraints/parameters	4883/0/370	5097/0/380
Goodness-of-fit on F^2	1.081	1.018
Final R indices [$I > 2\sigma(I)$]	$R1 = 0.0499$	$R1 = 0.0581$
	$wR2 = 0.0779$	$wR2 = 0.1513$
R indices (all data)	$R1 = 0.1347$	$R1 = 0.0628$
	$wR2 = 0.1481$	$wR2 = 0.1560$

$R1 = [|F_o| - |F_c|]/|F_o|$.
$wR2 = [w(F_o^2 - F_c^2)^2]/[w(F_o^2)^2]^{1/2}$.

Table 2. Selected bond lengths (Å) and angles (°) for **1** and **2**.

Complex **1**			
Zn(1)–O(2)	1.965(5)	Zn(1)–N(1)	2.084(5)
Zn(1)–O(3)	1.959(4)	Zn(1)–N(2)	2.092(5)
O(3)–Zn(1)–O(2)	129.7(2)	O(3)–Zn(1)–N(2)	105.67(19)
O(3)–Zn(1)–N(1)	107.20(19)	O(2)–Zn(1)–N(2)	114.7(2)
O(2)–Zn(1)–N(1)	107.7(2)	N(1)–Zn(1)–N(2)	80.8(2)
Complex **2**			
Zn(1)–O(1)	1.938(3)	Zn(1)–N(3)	2.073(3)
Zn(1)–O(3)	1.953(3)	Zn(1)–N(4)	2.076(3)
O(3)–Zn(1)–N(3)	95.15(11)	O(1)–Zn(1)–N4)	97.34(13)
N(3)–Zn(1)–N(4)	116.69(12)	O(1)–Zn(1)–N(3)	105.80(13)
O(3)–Zn(1)–N(4)	103.64(12)	O(1)–Zn(1)–O(3)	139.53(13)

and Hg^{2+}, and nitrates of Ag^{+} and Pb^{2+}. Standard solutions of Hg^{2+} at different concentrations were obtained by serial dilution of 1.0×10^{-5} mol dm^{-3} $HgCl_2$ solution. A 1.0×10^{-5} mol dm^{-3} stock solution of **1** or **2** was prepared by dissolving them in DMF and then diluting in water. The ratio of DMF and H_2O is 1 : 100 (v/v). The aforementioned solution of Hg^{2+} and **1** or **2** stock solution are titrated in a 1/1 (v/v) ratio for subsequent fluorescence measurement. The solution samples were measured in a 1.00 cm quartz cell. Chloride salts of Ag^{+} and Pb^{2+} are not soluble in water, so we used nitrates. We also investigated the influence of anions on fluorescence of **1** or **2**. The results revealed that NO_3^- and Cl^- did not influence the fluorescence.

3. Results and discussion

3.1. *Synthesis*

Self-assembly of IAH with metal ions in the dark is an effective route for the growth of single crystals of coordination complexes containing indole-3-acetate. IAH is easily decomposed by light, heat, and oxygen, with a complicated photoisomerization reaction, generating a new rose-colored material [18]. If the mixture of IAH and metal ions in ethanol was under light, it rapidly yields brown precipitate, whose composition cannot be identified. Thus, crystals suitable for X-ray crystallography for **1** and **2** were grown by slow evaporation of their methanol solutions in the dark.

Only when bipyridine-based ligands (4,4′-bipy or phen) were added, IA^- could be induced to form **1** and **2**. Reported crystal structures based on indole-3-acetate only include [Pb(IA)$_2$(phen)] [19] and 1-D chain [Co(IA)$_2$(4,4′-bipy)(H$_2$O)$_2$] · 4H$_2$O [20], both of which also include auxiliary ligands phen and 4,4′-bipy, respectively. There is no reported crystal structure of a coordination complex with only IA^- and metal ions, although many metal indole-3-acetate coordination complexes have been synthesized and found to possess interesting properties [21, 22].

Both complexes are air stable for long times and soluble in DMF or DMSO, but not soluble in common organic solvents, such as MeOH, EtOH, MeCN, and THF.

3.2. *The crystal structures of 1 and 2*

Single-crystal X-ray diffraction reveals that **1** crystallizes in the monoclinic space group $P2_1/c$. The overall view and labeling of the atoms in **1** are displayed in figure 1.

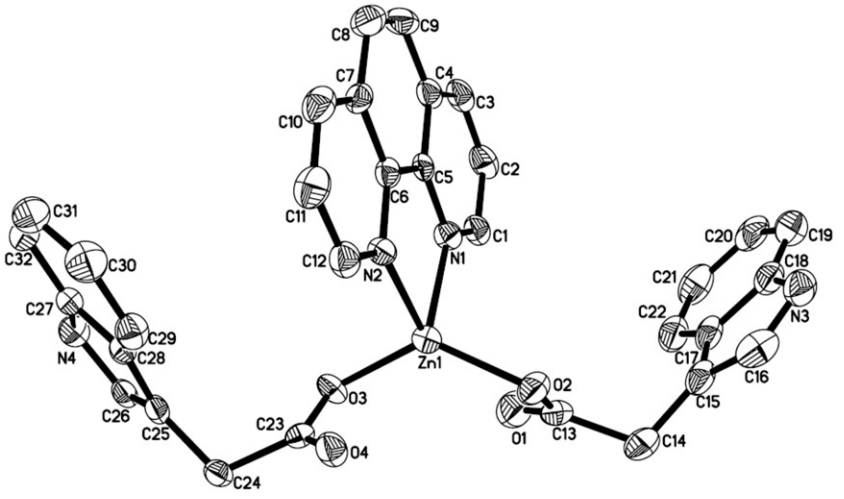

Figure 1. ORTEP view of **1** with full-labeling scheme. The ellipsoids enclose 30% of the electronic density.

Complex **1** is mononuclear and its structure looks like a butterfly, similar to that of $[Pb(IA)_2(phen)]$ [19]. Each Zn(II) is coordinated by two IA and one phen, featuring a slightly distorted tetrahedral geometry. The bond lengths of Zn–O are 1.958(4) and 1.964(5) Å and Zn–N are 2.090(5) and 2.082(5) Å. In **1**, the phen chelates Zn^{2+} and the two IA ligands lie on both sides of the phen with angle of 51.973° between them. Both IA ligands in **1** are almost coplanar with dihedral angle of 0.807°, respectively, so does the phen with dihedral angle of 0.416°. In the solid state of **1**, there exist N–H···O hydrogen-bonding interactions involving oxygen and nitrogen from IA, and the N–H···O distance is 2.834 Å, shorter than reported N–H···O hydrogen bonds [23]. The existence of the hydrogen bonds makes the structure more stable.

Complex **2** is a 1-D zigzag chain polymer of $[Zn_2(IA)_4]$ bridged by 4,4′-bipy, similar to that of $[Co(IA)_2(4,4'\text{-bipy})(H_2O)_2]\cdot 4H_2O$ [20]. It crystallizes in the monoclinic space group $P2_1/c$ (figure 2). As shown in figure 3 [24], each Zn(II) has a distorted tetrahedral geometry with two oxygens from two IA and one nitrogen from one 4,4′-bipy with the average Zn–O and Zn–N bond lengths at 1.945 and 2.076 Å, respectively. The Zn(II) ions are bridged by 4,4′-bipy, forming ···Zn···4,4′-bipy···Zn···4,4′-bipy··· zigzag chain, in which the Zn···Zn distance is 11.189 Å. In the chain, the two pyridyl rings in 4,4′-bipy ligand are strictly coplanar (the dihedral angle is 0°), while the benzopyrrole rings of IA are not coplanar with a dihedral angle of 0.692°.

As shown in figure 4, the chains are arranged with intermolecular interaction parallel in the *ab* plane leading to pseudo structural sheets. These pseudo structural sheets are parallel and stack along the *c*-axis with a rotation; the packing mode of the chains is shown in figure 4(b). The 1-D chains lying in adjacent consecutive sheets extend along two different directions and directly complete high-dimensional supramolecular assembly through N–H···O hydrogen bonds from IA ligands in adjacent chains. The length of N–H···O hydrogen bonds is 2.817 Å, shorter than that of **1**, and the angle of N–H···O is 152.2°. Furthermore, free lattice C_2H_5OH resides in adjacent sheets and are hydrogen-bonded to IA (O–H···O = 2.885 Å), which suggests strong intermolecular interactions.

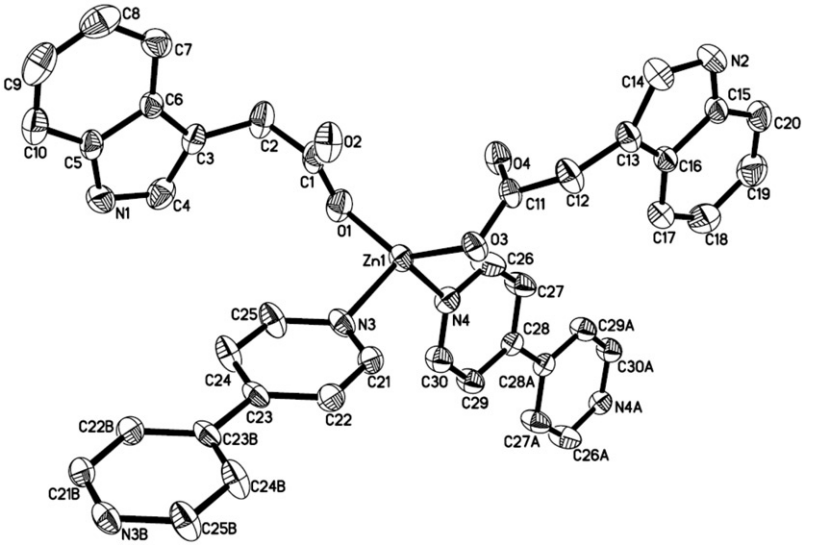

Figure 2. ORTEP view of **2** with full-labeling scheme. The ellipsoids enclose 30% of the electronic density (lattice ethanols have been omitted for clarity).

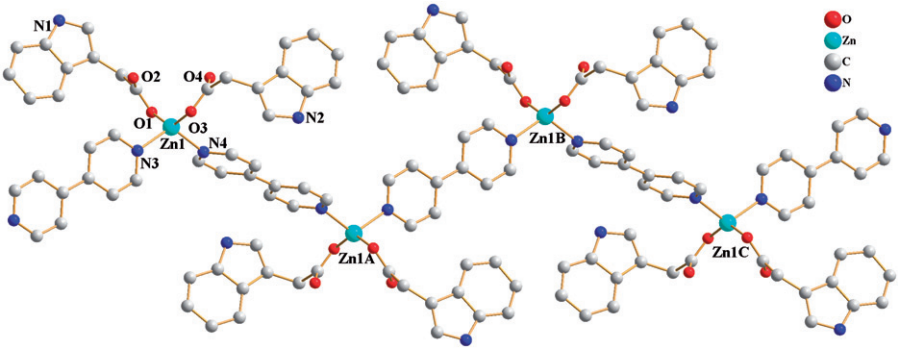

Figure 3. The 1-D zigzag chain of **2** (lattice ethanols have been omitted for clarity).

IAH has nitrogens and carboxylates, which are favorable to coordinate to metals, terminal monodentate, bidentate, and *O,O′*-bridging. Supramolecular structures may be formed by π–π interactions between indole rings. Thus, one can expect IAH to be an asymmetric bridging ligand coordinating with metal ions forming 1-D or high-dimensional structures. However, IAH is terminal in **1** and **2**, as well as [Pb(IA)$_2$(phen)] [19] and [Co(IA)$_2$(4,4′-bipy)(H$_2$O)$_2$] · 4H$_2$O [20], rather than end-to-end bridging groups since the nitrogen of indole is not involved in coordination; only one oxygen in IA ligand is involved in coordination. Nitrogens in phen and 4,4′-bipy are better donors than that of indole ring in IA, thus two nitrogens in phen and 4,4′-bipy coordinated with zinc, but nitrogen in indole does not coordinate [25].

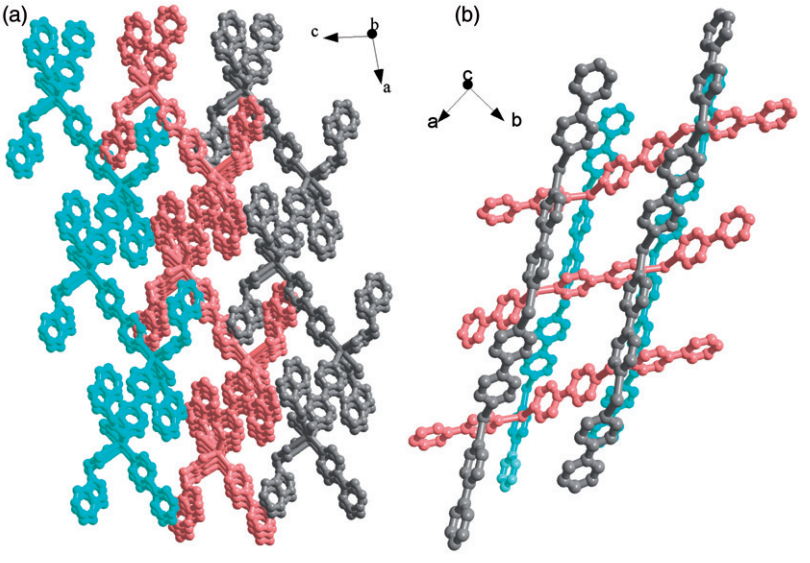

Figure 4. The packing mode of 1-D infinite chains of **2** viewed from (a) *b* and (b) *c* directions (hydrogens have been omitted for clarity).

3.3. *Selective luminescent responses of 1 and 2 to various metal ions*

The investigation of fluorescence response behaviors showed that both **1** and **2** exhibited satisfactory fluorescence emissions in DMF/H_2O solution, giving the same emission maximum at 360 nm.

The fluorescence behaviors of **1** and **2** toward different metal ions were investigated by interaction with 1.0×10^{-5} mol dm^{-3} of alkali (Na^+, K^+), alkaline earth (Mg^{2+}, Ca^{2+}), and transition-metal ions (Mn^{2+}, Cr^{3+}, Fe^{3+}, Ni^{2+}, Cd^{2+}, Co^{2+}, Cu^{2+}, Hg^{2+}, Ag^+), and Pb^{2+}. Upon addition of different cations, the emission spectrum exhibits excellent fluorescence selectivity toward Hg^{2+}, namely fluorescence quenching, while other metal ions only caused slight intensity changes (figure 5a). The fluorescence behavior of **2** toward the metal ions was similar to that of **1**, also generating effective recognition of Hg^{2+} (figure 5b).

The fluorescence response behavior of the two complexes on Hg^{2+} has been investigated. Figure 6 shows fluorescence spectra of **1** (a) and **2** (b) (1.0×10^{-5} mol dm^{-3}) in aqueous solution upon addition of Hg^{2+} from 1.0×10^{-6} to 10×10^{-6} mol dm^{-3}. They both show a gradual decrease in fluorescence as the concentration of Hg^{2+} increased from 1.0×10^{-6} to 10×10^{-6} mol dm^{-3}, indicating that the fluorescence emission of the complexes was quenched by the addition of Hg^{2+}. Generally, the design of fluorescent chemosensors is based on photo-induced electron/energy transfer (PET) [26], metal–ligand charge transfer (MLCT) [27], intramolecular charge transfer (ICT) [28], excimer/exciplex formation [29], guest-induced changes in the rigidity of the host molecules [30–32], etc. We consider that the quenching effect of fluorescence may be attributed to ligand–metal charge transfer (LMCT) mechanism in which electronic charge is transferred from the complex toward the metal ion [33]. In our experiment, the electronic charge of the complexes (N and O) transferred to

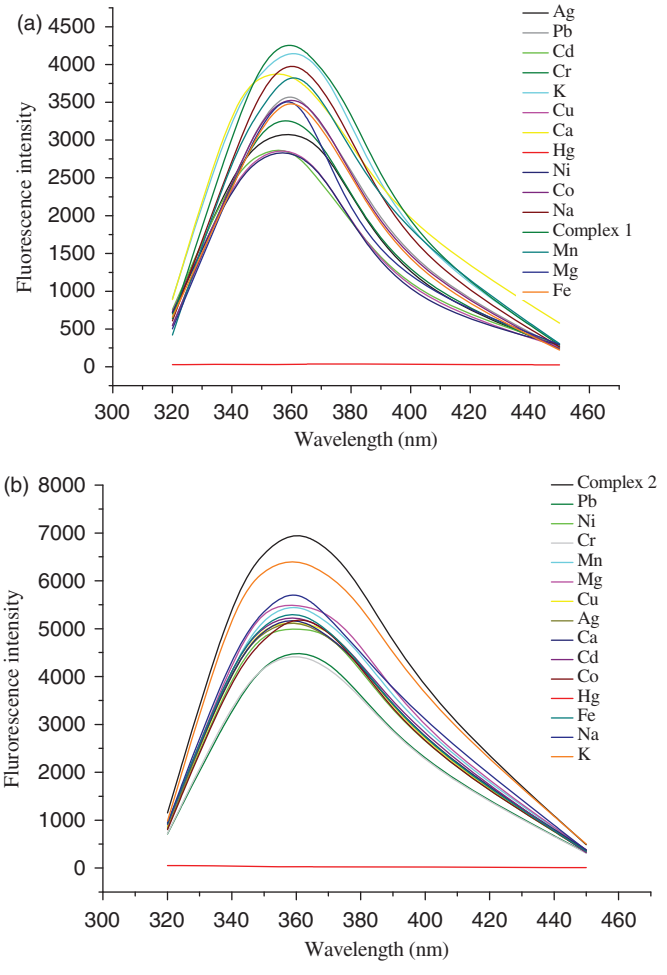

Figure 5. Fluorescence spectra of (a) **1** and (b) **2** (1.0×10^{-5} mol dm^{-3}) with addition of Na^+, K^+, Mg^{2+}, Ca^{2+}, Cr^{3+}, Mn^{2+}, Fe^{3+}, Co^{2+}, Ni^{2+}, Cu^{2+}, Cd^{2+}, Hg^{2+}, Ag^+, and Pb^{2+} (1 equiv, respectively) in 99% DMF aqueous media with an excitation at 297 nm.

Hg^{2+} (d-orbital) and the electronic charge of the complexes was redistributed in an excited state, which resulted in fluorescence quenching of the complexes [34].

Moreover, the detection limits for Hg^{2+} were found to be 1.0×10^{-5} mol dm^{-3} for **1** and **2**, both of which exhibit Hg^{2+}-specific fluorescence quenching over various competitive cations, including alkali and alkali earth, first-row transition metals and heavy metals. To the best of our knowledge, metal–organic complexes are rarely reported as fluorescence probes for selective detection of Hg^{2+}. Most Hg^{2+}-selective fluorescence sensors are designed as organic compounds, such as calixarene [35], crown ethers [36, 37], hydroxyquinolines [38, 39], azines [40], cyclams [41, 42], and rhodamine compounds [43, 44], which contain nitrogen, oxygen, and sulfur to coordinate Hg^{2+}. However, some of these sensors have drawbacks in terms of synthetic difficulty, high cost of starting materials or lack of selectivity. In comparison, **1** and **2** can be easily synthesized and show high sensitivity and selectivity toward Hg^{2+} over a wide range

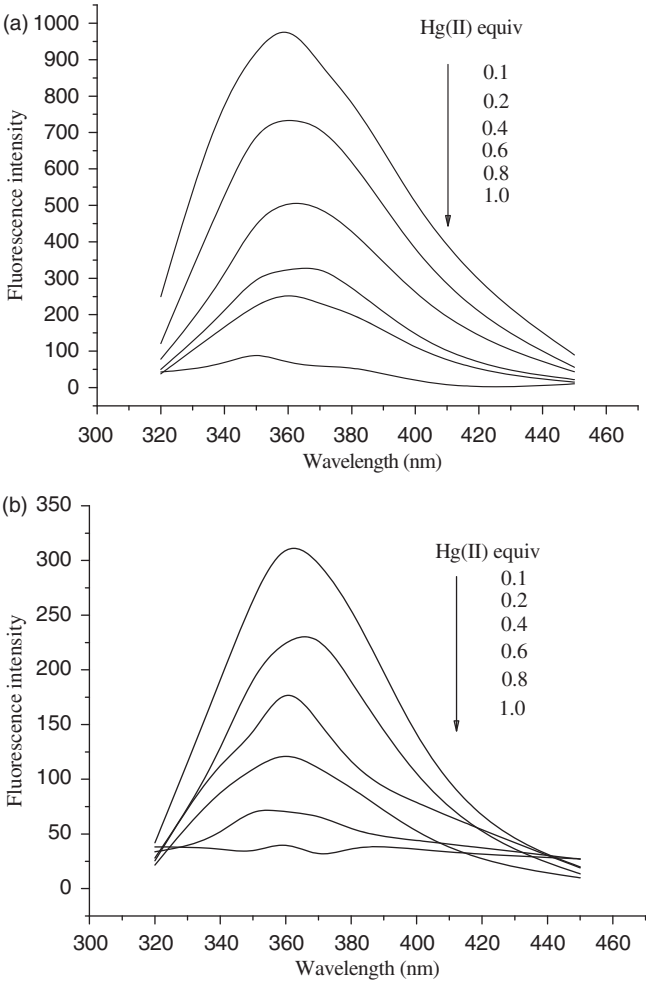

Figure 6. The emission response of (a) **1** and (b) **2** (both in 1.0×10^{-5} mol dm^{-3}) to different concentrations of Hg^{2+} (1.0, 2.0, 4.0, 6.0, 8.0, 10.0×10^{-6} mol dm^{-3}) in 99% DMF aqueous media with excitation at 297 nm.

of metal ions, making the two complexes practical Hg^{2+}-selective fluorescence sensors in aqueous systems.

3.4. *Hg^{2+}-exchanged products of 1 and 2*

To better understand the behavior of the two complexes with Hg^{2+}, we immersed 10.0 mg block crystals of as-synthesized **1** and **2** into an aqueous solution of 0.01 mol dm^{-3} mercury chloride (10 cm^3). Both **1** and **2** do not dissolve in water. After 1 month, the immersed block crystals of **1** break into opaque slivers and **2** changed into very fine needles.

EDS measurements were carried out on the Hg-exchanged products of **1** and **2**. The SEM and EDS results, depicted in figures 7 and 8, show that the detected surface and

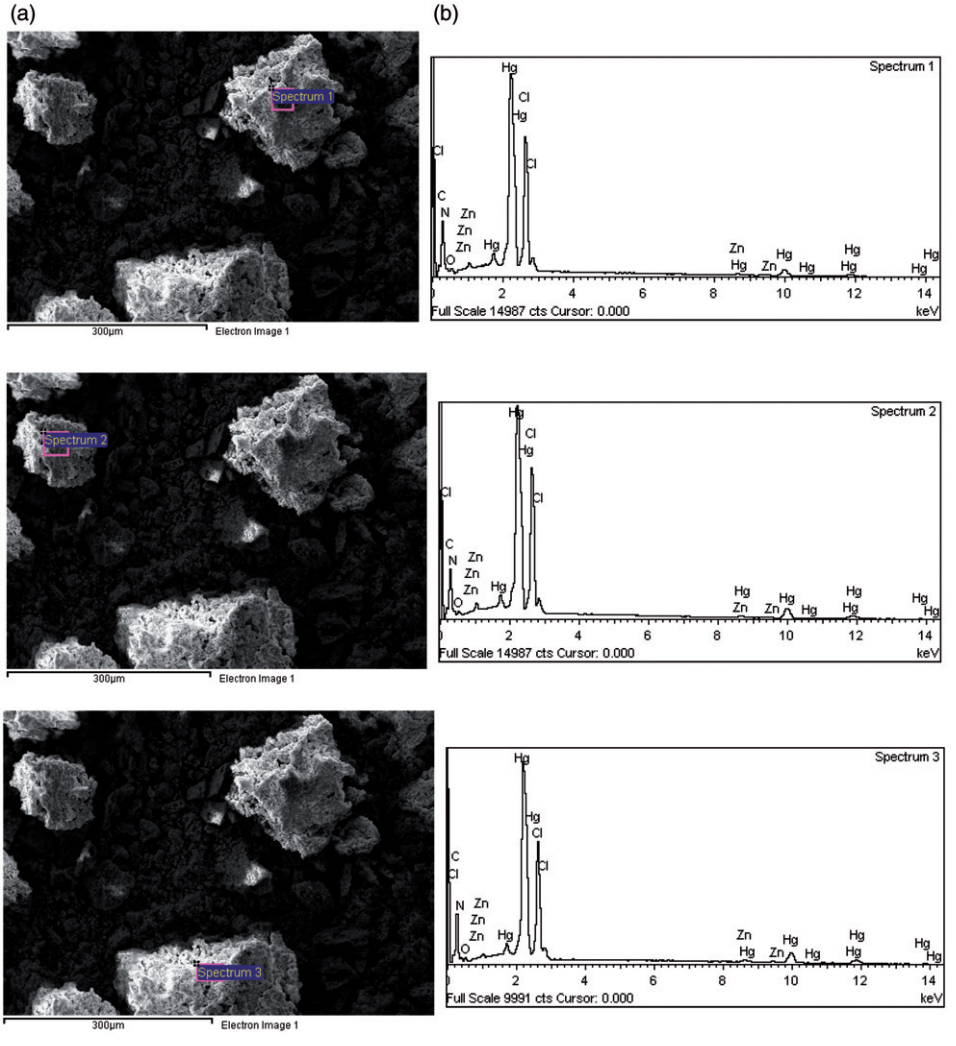

Figure 7. (a) SEM and (b) EDS for the surface and interior after substitution of **1** with mercury ion.

average interior atom ratios for carbon, nitrogen, oxygen, chlorine, zinc, and mercury are 73.63%, 8.97%, 3.02%, 9.39%, 0.29%, and 4.70%, respectively (for **1**); 79.75%, 1.98%, 4.22%, 8.36%, 0.18%, and 5.51%, respectively (for **2**). Obviously, zinc contents decreased dramatically from 11.0% (according to elemental analyses) to 0.29% (for **1**) and from 10.6% (according to elemental analyses) to 0.18% (for **2**), and there were high mercury contents in both cation-exchanged products of **1** and **2**. To ascertain the cation-exchanged mechanism, we determined the concentration of zinc ion in aqueous solution by ICP. It was found that the concentrations of zinc ion increased from 0.0 to 49 and 68 ppm in **1** and **2**, respectively. Thus, it can be confirmed that **1** and **2** could adsorb mercury ions by ion-exchange mechanism.

Considering the fluorescence quench of **1** and **2** with addition of Hg^{2+}, we determined the fluorescence of Hg-exchanged products of **1** and **2**. The result was as anticipated as

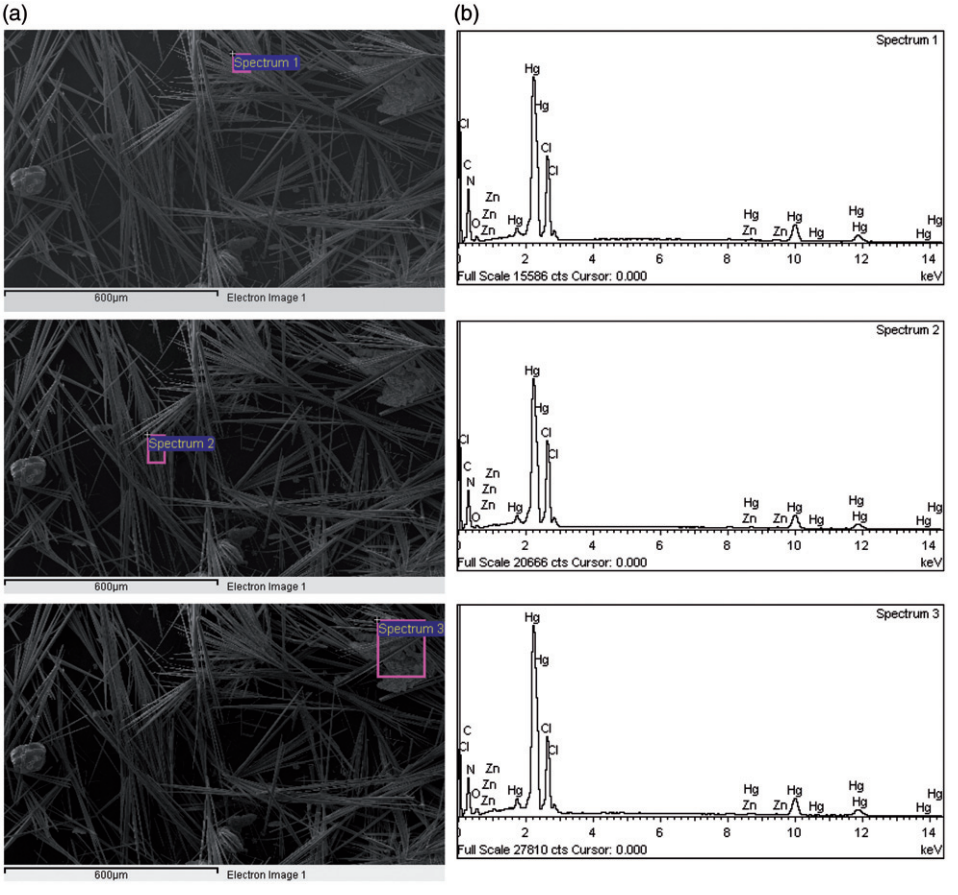

Figure 8. (a) SEM and (b) EDS for the surface and interior after substitution of **2** with mercury ion.

both exchanged products have no fluorescence, consistent with the selective luminescent responses of **1** and **2** to mercury. Cation-exchange reaction between zinc and mercury can also occur in solutions, resulting in change of fluorescence intensity of **1** and **2**.

4. Conclusion

Two new and simple fluorescence sensors of zinc(II) complexes for Hg^{2+} detection have been designed and structurally characterized that have advantage of sensitivity, selectivity, and synthetic simplicity. Hg^{2+}-selective fluorescence quenching of **1** and **2** were observed in aqueous dimethylformamide solutions with detection limit of 1.0×10^{-5} mol dm^{-3}. EDS and ICP results show that the zinc ions in the two complexes can exchange mercury from solution and release zinc, which is helpful to the environment. Considering beneficence to the plants and high sensing specificity for Hg^{2+} over other cations, the two complexes are expected to have applications to meet

the detection requirements of an Hg^{2+} assay in environmental fields. Further research on cation-exchange reactions is underway in our laboratory.

Supplementary material

Crystallographic data reported in this article have been deposited with the Cambridge Crystallographic Data Center as supplementary publication. CCDC numbers are 778970 for **1** and 778971 for **2**. These data can be obtained free of charge *via* www.ccdc.cam.ac.uk/conts/retrieving.htm (or from the Cambridge Crystallographic Data Centre, 12, Union Road, Cambridge CB2 1EZ, UK; Fax: +44 1223 336033).

Acknowledgments

The authors acknowledge financial support from the Education Department of Henan Province (2010A150025), the Science and Technology Projects of Zhengzhou 27 District (No. 20103376), and the Research Fund for Graduate of Zheng Zhou University (A0307).

References

[1] J.B. Wang, X.H. Qian. *J. Chem. Commun.*, 109 (2006).
[2] D. Obrist, A.G. Hallar, I. McCubbin, B.B. Stephens, T. Rahn. *Atmos. Environ.*, **42**, 7579 (2008).
[3] X.F. Guo, X.H. Qian, L.H. Jia. *J. Am. Chem. Soc.*, **126**, 2272 (2004).
[4] Y.K. Yang, K.J. Yook, J. Tae. *J. Am. Chem. Soc.*, **127**, 16760 (2005).
[5] A. Caballero, R. Martínez, V. Lloveras, I. Ratera, J. Vidal-Gancedo, K. Wurst, A. Tárraga, P. Molina, J. Veciana. *J. Am. Chem. Soc.*, **127**, 15666 (2005).
[6] D. Jimenez, R. Martínez-Manez, F. Sancenon, J. Soto. *Tetrahedron Lett.*, **45**, 1257 (2004).
[7] (a) M.Y. Chae, A.W. Czarnik. *J. Am. Chem. Soc.*, **114**, 9704 (1992); (b) G. Hennrich, H. Sonnenschein, U.R. Genger. *J. Am. Chem. Soc.*, **121**, 5073 (1999); (c) K. Rurack, M. Kollmannsberger, U.R. Genger, J. Daub. *J. Am. Chem. Soc.*, **122**, 968 (2000); (d) L. Prodi, C. Bargossi, M. Montalti, N. Zaccheroni, N. Su, J.S. Bradshaw, R.M. Izatt, P.B. Savage. *J. Am. Chem. Soc.*, **122**, 6769 (2000); (e) P. Pallavicini, Y.A. Diaz-Fernandez, F. Foti, C. Mangano, S. Patroni. *Chem. Eur. J.*, **13**, 178 (2007); (f) S. Yoon, E.W. Miller, Q. He, P.H. Do, C.J. Chang. *Angew. Chem., Int. Ed.*, **46**, 6658 (2007).
[8] (a) C.C. Huang, Z. Yang, K.H. Lee, H.T. Chang. *Angew. Chem. Int. Ed.*, **46**, 6824 (2007); (b) G.K. Darbha, A. Ray, P.C. Ray. *ACS Nano.*, **1**, 208 (2007).
[9] J.M. Thomas, R. Ting, D.M. Perrin. *Org. Biomol. Chem.*, **2**, 307 (2004).
[10] (a) P. Chen, C. He. *J. Am. Chem. Soc.*, **126**, 728 (2004); (b) J. Liu, Y. Lu. *Angew. Chem. Int. Ed.*, **46**, 7587 (2007).
[11] (a) A. Ono, H. Togashi. *Angew. Chem. Int. Ed.*, **43**, 4300 (2004); (b) X.F. Liu, Y.L. Tang, L.H. Wang, J. Zhang, S.P. Song, C.H. Fan, S. Wang. *Adv. Mater.*, **19**, 1471 (2007); (c) M.N. Schwemlein, W. Gilbert, K. Askew, S. Schwemlein. *Bioorg. Med. Chem.*, **16**, 5778 (2008).
[12] Y.L. Tang, F. He, M.H. Yu, F.D. Feng, L.L. An, H. Sun, S. Wang, Y.L. Li, D.B. Zhu. *Macromol. Rapid Commun.*, **27**, 389 (2006).
[13] Y.A. Son, J.H. Hwang, S. Wang, J.S. Bae, S.H. Kim. *Fibers Polym.*, **10**, 272 (2009).
[14] Y. Liu, M. Yu, Y. Chen, N. Zhang. *Bioorg. Med. Chem.*, **17**, 3887 (2009).
[15] R. Joseph, A. Gupta, C.P. Rao. *J. Photochem. Photobiol., A*, **188**, 325 (2007).
[16] Molecular Structure Corporation & Rigaku CrystalClear MSC, The Woodlands, Texas, USA, and Rigaku Corporation, Tokyo, Japan (2006).

[17] G.M. Sheldrick. *SHELX-97, Program for the Solution and Refinement of Crystal Structures*, University of Göttingen, Germany (1997).
[18] Z.L. Jiang, X.H. Liu, Z.Q. Wu, F. Li, C.W. Jiang. *J. Guangxi Norm. Univ*., **17**, 69 (1999).
[19] Z.F. Chen, L. Huang, R.X. Hu, S.M. Shi, H. Liang, Y. Li. *Appl. Organomet. Chem*., **19**, 211 (2005).
[20] J.W. Liu, S.W. Ng. *Acta Crystallogr., Sect. E*, **64**, 706 (2008).
[21] H.M. Liu, S.L. Niu, L. Shen, Y. Zhao. *J. Hebei Norm. Univ. Sci. Technol*., **22**, 29 (2008).
[22] M. Takani, H. Masuda, O. Yamauchi. *Inorg. Chim. Acta*, **235**, 367 (1995).
[23] M.A. Bensegueni, A. Cherouana, L. Bendjeddou, C. Lecomte, S. Dahaoui. *Acta Cryst*., **C65**, o607 (2009).
[24] K. Brandenburg. Diamond-Visual Crystal Structure Information System, *Version 2.1e*, Crystal Impact, Bonn, Germany (2001).
[25] Z.G. Song, S.X. Zhuang. *J. Nor. Norm. Univ. Nat. Sci*., **139**, 58 (2003).
[26] T. Gunnlaugsson, A.P. Davis, J.E. O'Brien, M. Glynn. *Org. Lett*., **4**, 2449 (2002).
[27] P.D. Beer. *Acc. Chem. Res*., **31**, 71 (1998).
[28] V. Thiagarajan, P. Ramamurthy. *J. Lumin*., **126**, 886 (2007).
[29] J.S. Wu, J.H. Zhou, P.F. Wang, X.H. Zhang, S.K. Wu. *Org. Lett*., **7**, 2133 (2005).
[30] S. Watanabe, O. Onogawa, Y. Komatsu, K. Yoshida. *J. Am. Chem. Soc*., **120**, 229 (1998).
[31] Z.H. Lin, Y.G. Zhao, Ch.Y. Duan, B.G. Zhang, Z.P. Bai. *Dalton Trans*., **36**, 78 (2006).
[32] J. Bourson, J. Pouget, B. Valeur. *J. Phys. Chem*., **97**, 4552 (1993).
[33] D.X. Zeng, Y. Chen. *J. Photochem. Photobiol. A*, **186**, 121 (2007).
[34] Y. Liu, M. Yu, Y. Chen, N. Zhang. *Bioorg. Med. Chem*., **17**, 3887 (2009).
[35] R. Metivier, I. Leray, B. Valeur. *Chem. Eur. J*., **10**, 4480 (2004).
[36] E.R. Carraway, N. Demas, B.A.D. Degraff. *Anal. Chem*., **63**, 337 (1991).
[37] Q. Zhao, S.J. Liu, F.Y. Li, T. Yi, C.H. Huang. *Dalton Trans*., 3836 (2008).
[38] S.Y. Moon, N.R. Cha, Y.H. Kim, S.K. Chang. *J. Org. Chem*., **69**, 181 (2004).
[39] H. Zhang, L.F. Han, K.A. Zachariasse, Y.B. Jiang. *Org. Lett*., **7**, 4217 (2005).
[40] R. Martinez, A. Espinosa, A. Tarraga, P. Molina. *Org. Lett*., **7**, 5869 (2005).
[41] S.M. Park, M.H. Kim, J.I. Choe, K.T. No, S.K. Chang. *J. Org. Chem*., **72**, 3550 (2007).
[42] S.H. Kim, J.S. Kim, S.M. Park, S.K. Chang. *Org. Lett*., **8**, 371 (2006).
[43] W. Huang, C.X. Song, C. He, G.J. Lv, X.Y. Hu, X. Zhu, C.Y. Duan. *Inorg. Chem*., **48**, 5061 (2009).
[44] X.L. Zhang, Y. Xiao, X.H. Qian. *Angew Chem. Int. Ed*., **47**, 8025 (2008).